J|A|C|S
ARTICLES
Published on Web 03/15/2002

Second-Sphere Contributions to Substrate-Analogue Binding in Iron(III) Superoxide Dismutase

Juan Xie, Emine Yikilmaz,[§] Anne-Frances Miller,*[,§] and Thomas C. Brunold*

Contribution from the Department of Chemistry, University of Wisconsin-Madison, Madison, Wisconsin 53706, and Department of Chemistry, University of Kentucky, Lexington, Kentucky 40506

Received May 23, 2001

Abstract: A combination of spectroscopic and computational methods has been employed to explore the nature of the yellow and pink low-temperature azide adducts of iron(III) superoxide dismutase (N_3−FeSOD), which have been known for more than two decades. Variable-temperature variable-field magnetic circular dichroism (MCD) data suggest that both species possess similar ferric centers with a single azide ligand bound, contradicting previous proposals invoking two azide ligands in the pink form. Complementary data obtained on the azide complex of the Q69E FeSOD mutant reveal that relatively minor perturbations in the metal-center environment are sufficient to produce significant spectral changes; the Q69E N_3−FeSOD species is red in color at all temperatures. Resonance Raman (RR) spectra of the wild-type and Q69E mutant N_3−FeSOD complexes are consistent with similar Fe−N_3 units in all three species; however, variations in energies and relative intensities of the RR features associated with this unit reveal subtle differences in (N_3^-)−Fe^{3+} bonding. To understand these differences on a quantitative level, density functional theory and semiempirical INDO/S-CI calculations have been performed on N_3−FeSOD models. These computations support our model that a single azide ligand is present in all three N_3−FeSOD adducts and suggest that their different appearances reflect differences in the Fe−N−N bond angle. A 10° increase in the Fe−N−N bond angle is sufficient to account for the spectral differences between the yellow and pink wild-type N_3−FeSOD species. We show that this bond angle is strongly affected by the second coordination sphere, which therefore might also play an important role in orienting incoming substrate for reaction with the FeSOD active site.

1. Introduction

Superoxide dismutases (SODs) defend biological systems against oxidative damage mediated by the superoxide radical anion ($O_2^{\bullet-}$).[1] Several distinct SODs are known with Mn-, Fe-, Cu/Zn-, or Ni-containing active sites.[1,2] While the Mn- and Fe-dependent SODs are homologous, they are unrelated to the other SODs. Mn- and FeSODs accomplish their function through disproportionation of $O_2^{\bullet-}$ to O_2 and H_2O_2 according to eqs 1 and 2.[3,4] In this mechanism, the metal ion M (corresponding to manganese or iron) cycles between its +3 and +2 oxidation states.

$$M^{3+}-SOD + O_2^{\bullet-} \rightarrow M^{2+}-SOD + O_2 \quad (1)$$

$$M^{2+}-SOD + O_2^{\bullet-} + 2H^+ \rightarrow M^{3+}-SOD + H_2O_2 \quad (2)$$

Even though the Mn- and FeSODs from *Escherichia coli* share the same basic protein fold and possess virtually identical active site structures,[5] these enzymes are metal specific; that is, neither Mn-substituted FeSOD nor Fe-substituted MnSOD displays catalytic activity.[1,6,7] This extraordinary specificity has been proposed to arise from subtle differences in the second coordination sphere that strongly affect the reduction midpoint potential, E_m, of the bound metal ion.[1,7,8] By using a combination of spectroscopic and computational techniques in conjunction with site-directed mutagenesis, we were able to show that the conserved active-site Gln (corresponding to positions 146 and 69 in MnSOD and FeSOD, respectively) exerts significant control over E_m by modulating the pK_a of the metal-bound solvent ligand to which it is hydrogen-bonded.[9] Substitution of this Gln by Glu, which is isosteric and isoelectronic to Gln but functions as an H-bond acceptor instead of an H-bond donor, raises the E_m of FeSOD by several hundred millivolts, most likely because this mutation greatly increases the stability of coordinated H_2O in the reduced state.[9]

[§] University of Kentucky.

(1) Miller, A. F.; Sorkin, D. L. *Comments Mol. Cell. Biophys.* **1997**, *9*, 1−48.
(2) Choudhury, S. B.; Lee, J. W.; Davidson, G.; Yim, Y. I.; Bose, K.; Sharma, M. L.; Kang, S. O.; Cabelli, D. E.; Maroney, M. J. *Biochemistry* **1999**, *38*, 3744−3752.
(3) Bull, C.; Fee, J. A. *J. Am. Chem. Soc.* **1985**, *107*, 3295−3304.
(4) Bull, C.; Niederhoffer, E. C.; Yoshida, T.; Fee, J. A. *J. Am. Chem. Soc.* **1991**, *113*, 4069−4076.
(5) Lah, M. S.; Dixon, M. M.; Pattridge, K. A.; Stallings, W. C.; Fee, J. A.; Ludwig, M. L. *Biochemistry* **1995**, *34*, 1646−1660.
(6) (a) Vance, C. K.; Miller, A.-F. *J. Am. Chem. Soc.* **1998**, *120*, 461−467. (b) Vance, C. K.; Miller, A. F. *Biochemistry* **2001**, *40*, 13079−13087.
(7) (a) Ose, D. E.; Fridovich, I. *J. Biol. Chem.* **1976**, *251*, 1217−1218. (b) Yamakura, F. *J. Biochem.* **1978**, *83*, 849−857.
(8) Miller, A. F. In *Handbook of Metalloproteins*; Messerschmidt, A., Huber, R., Poulos, T., Wieghardt, K., Eds.; John Wiley & Sons: Chichester, 2001; pp 668−682.
(9) Yikilmaz, E.; Xie, J.; Brunold, T. C.; Miller, A. F. *J. Am. Chem. Soc.* **2002**, *124*, 3482−3483.

10.1021/ja016254h CCC: $22.00

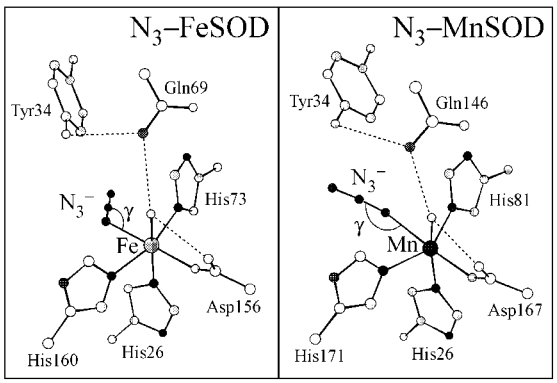

Figure 1. Active sites of N_3-FeSOD (left) and N_3-MnSOD (right), based on the coordinates of Lah et al.;[5] protein database files 1ISC and 1MNG. The conserved hydrogen-bond networks involving the metal-bound solvent ligand are indicated by the broken lines.

Fe- and MnSODs are competitively inhibited by azide (N_3^-),[1,3,8] a close mimic of the $O_2^{\bullet-}$ substrate with respect to charge and "frontier" orbitals that are involved in bonding to the metal center.[10] Azide binds to the five-coordinate Fe^{3+} and Mn^{3+} active sites of the resting proteins to yield six-coordinate complexes at low temperatures that have been characterized using crystallographic and spectroscopic methods (Figure 1).[5,11−15] In N_3-MnSOD, the metal−N−N angle is $\gamma = 147°$, and the N_3^- ligand appears to H-bond to the universally conserved second-sphere Tyr. By contrast, in N_3-FeSOD this angle is only $\gamma = 117°$, and N_3^- is directed away from this Tyr residue. Variable-temperature absorption data on N_3-MnSOD appear to indicate that a five-coordinate N_3^- complex is formed at physiological temperatures (the identity of the displaced ligand is not yet known),[14,15] whereas the ferric site of N_3-FeSOD is probably six-coordinate at all temperatures.[5,13] However, two distinct N_3^- complexes can be obtained for Fe^{3+}SOD upon freezing: a pink complex (obtained at low protein concentrations and $[N_3^-]/[Fe^{3+}SOD] > 2$) and a yellow species (obtained in all other instances), that were tentatively assigned to six-coordinate N_3-Fe^{3+}SOD complexes with two and one azide ligands bound, respectively.[16] While the distinct interactions of MnSOD and FeSOD with the substrate analogue azide are intriguing, possibly reflecting differences in the corresponding catalytic mechanisms, it remains to be shown whether these differences are due solely to the different intrinsic reactivities of the active-site metal ions.

In the present study, magnetic circular dichroism (MCD) and resonance Raman (RR) spectroscopies are used in conjunction with density functional theory (DFT) and semiempirical INDO/S-CI calculations to elucidate the relationship between the geometric and electronic structures of the yellow and pink N_3-FeSOD species. Complementary data obtained on the azide complex of the Q69E FeSOD mutant reveal that alterations in the H-bond network involving the coordinated solvent (Figure 1) are sufficient to produce significant spectral changes, which can be correlated with perturbations in $Fe-N_3$ bonding. Our results suggest that the second coordination sphere, previously shown to be involved in redox tuning,[8,9,17] may also play an important role in orienting the incoming substrate for optimum catalytic performance.

2. Experimental Section

Protein Species. Wild-type FeSOD was overexpressed in *E. coli* and purified as described previously.[16,18] The specific activity was ~7000 units/mg of protein per minute, and the Fe content was ~2.2 Fe/protein dimer based on the absorbance at 350 nm and the published extinction coefficients.[16] The gene for Q69E FeSOD was constructed by polymerase chain reaction using the megaprimer method.[19] Both strands of the mutant gene were sequenced to confirm mutation of the CAG Gln codon to GAG for Glu, and to ascertain that no additional mutations had occurred. The mutant protein was expressed and isolated according to established procedures.[16,18] Consistent with the conservative nature of the amino acid substitution, the mutant was found to bind ~2 Fe/protein dimer (determined on the basis of a colorimetric assay[20] and atomic absorption measurements, and using the ϵ_{280} of FeSOD[16]), and to possess a wild-type-like active site structure both in the reduced and in the oxidized states.[9] However, the Q69E mutant is completely inactive, presumably because its E_m is too positive. Oxidized Q69E Fe^{3+}SOD protein was prepared by treatment of as-isolated (i.e., fully reduced) protein with 1 equiv of $KMnO_4$. Protein and azide concentrations used in our experiments are given in the figure captions.

Spectroscopy. Variable-temperature absorption, CD, and MCD spectra were recorded using a Jasco J-715 spectropolarimeter in conjunction with an Oxford Instruments SM-4000 8T magnetocryostat. All low-temperature CD and MCD data were taken in 50% (v/v) glycerol and 50 mM potassium phosphate buffer (pH 7.0). RR spectra were obtained upon excitation with an Ar^+ ion laser (Coherent I-305) in conjunction with a dye laser (Coherent 599-01, equipped with rhodamine 6G dye) using 5−25 mW laser power at the sample. Data were collected using an ~135° backscattering arrangement on samples contained in NMR tubes that were placed in an EPR dewar filled with liquid N_2 ($T = 77$ K). The scattered light was dispersed by a triple monochromator (Acton Research, equipped with 300, 1200, and 2400 gr/mm gratings) and detected with a back-illuminated CCD camera (Princeton Instruments, 1340 × 100 pixels).

Normal Coordinate Analysis. A normal coordinate analysis (NCA) of the vibrational data was performed on the $Fe-N_3$ unit characterized crystallographically: Fe−N = 2.12 Å, N−N = 1.15 Å, Fe−N−N angle $\gamma = 117°$, and N−N−N angle of 178° (obtained by averaging over the two subunits).[5] The analysis was based on the Wilson FG matrix method using a Urey−Bradley force field as implemented in a modified version[21] of the Schachtschneider program.[22]

Computations. The active site models for N_3-FeSOD employed in our computations were based on the protein database file 1ISC.[5] DFT calculations were carried out using the Amsterdam density functional (ADF) 2000.02 software package.[23−26] All geometry opti-

(10) Pate, J. E.; Ross, P. K.; Thamann, T. J.; Reed, C. A.; Karlin, K. D.; Sorrell, T. N.; Solomon, E. I. *J. Am. Chem. Soc.* **1989**, *111*, 5198−5209.
(11) Stallings, W. C.; Metzger, A. L.; Pattridge, K. A.; Fee, J. A.; Ludwig, M. L. *Free Radical Res. Commun.* **1991**, *12−13*, 259−268.
(12) Ludwig, M. L.; Metzger, A. L.; Pattridge, K. A.; Stallings, W. C. *J. Mol. Biol.* **1991**, *219*, 335−358.
(13) Tierney, D. L.; Fee, J. A.; Ludwig, M. L.; Penner-Hahn, J. E. *Biochemistry* **1995**, *34*, 1661−1668.
(14) Whittaker, M. M.; Whittaker, J. W. *Biochemistry* **1996**, *35*, 6762−6770.
(15) Whittaker, M. M.; Whittaker, J. W. *J. Biol. Inorg. Chem.* **1997**, *2*, 667−671.
(16) Slykhouse, T. O.; Fee, J. A. *J. Biol. Chem.* **1976**, *251*, 5472−5477.
(17) Schwartz, A. L.; Yikilmaz, E.; Vance, C. K.; Vathyam, S.; Miller, A.-F. *J. Inorg. Biochem.* **2000**, *80*, 247−256.
(18) Sorkin, D. L.; Miller, A.-F. *Biochemistry* **1997**, *36*, 4916−4924.
(19) Barik, S. In *Methods in Molecular Biology; PCR Cloning Protocols: From Molecular Cloning to Genetic Engineering*; White, B. A., Ed.; Humana Press: Totowa, NJ, 1989; pp 173−182.
(20) Carter, P. *Anal. Biochem.* **1971**, *40*, 450−458.
(21) Fuhrer, H.; Kartha, V. B.; Kidd, K. G.; Krueger, P. J.; Mantsch, H. H. Computer Programs for Infrared Spectroscopy, Bulletin No. 15, National Research Council of Canada, 1976.
(22) Schachtschneider, J. H. Technical Report No. 57-65, Shell Development Co., Emeryville, CA, 1966.
(23) Baerends, E. J.; Ellis, D. E.; Ros, P. *Chem. Phys.* **1973**, *2*, 41.
(24) Versluis, L.; Ziegler, T. *J. Chem. Phys.* **1988**, *88*, 322−328.
(25) te Velde, G.; Baerends, E. J. *J. Comput. Phys.* **1992**, *99*, 84−98.
(26) Guerra, C. F.; Snijders, J. G.; te Velde, G.; Baerends, E. J. *Theor. Chem. Acc.* **1998**, *99*, 391−403.

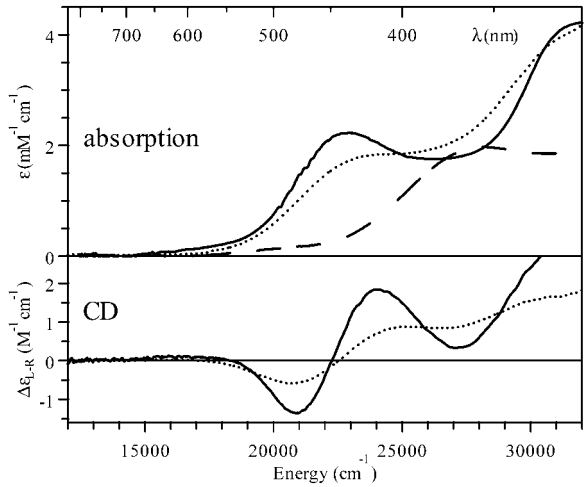

Figure 2. Absorption and CD spectra at 4.5 K (solid lines) and 300 K (dotted lines) of the yellow N_3−FeSOD adduct. The 300 K absorption spectrum of resting Fe^{3+}SOD is shown for comparison (broken line). Sample conditions: [Fe^{3+}SOD] = 1.4 mM, [NaN_3] = 100 mM in 50% (v/v) glycerol and 50 mM phosphate buffer (pH 7.0).

mizations were performed on a home-built cluster consisting of eight Pentium III processors using ADF basis set II, an integration constant of 4.0, and the Vosko, Wilk, Nusair local density approximation[27] with the nonlocal gradient corrections of Becke[28] and Perdew.[29] All semiempirical INDO/S-CI calculations on the DFT geometry-optimized N_3−FeSOD models were of the valence-only type and were performed using the electronic structure calculation package ORCA 2001 developed by Dr. Frank Neese (MPI Mülheim, Germany). ORCA utilizes the INDO/S model of Zerner and co-workers,[30,31] the valence shell ionization potentials and Slater−Condon parameters listed by Bacon and Zerner,[32] and the standard interaction factors $f_{p\sigma p\sigma} = 1.266$ and $f_{p\pi p\pi} = 0.585$. No changes in semiempirical parameters were found necessary for the present study. Restricted open-shell (ROHF) SCF calculations were tightly converged on the ^{6}A ground state, which served as the reference state for configuration interaction (CI) calculations. Stable results for the sextet spin states were obtained by including all possible single excitations within all 66 MOs (which include 36 doubly occupied MOs (DOMOs), 5 singly occupied MOs (SOMOs), and 25 virtual MOs), together with the double excitations from the highest 27 DOMOs into the SOMOs. Larger active spaces did not significantly change our results. For additional details on INDO/S-CI calculations using the ORCA software package, see ref 33 and literature cited therein.

3. Results and Analysis

Electronic Spectroscopy. Figure 2 shows absorption and CD spectra of the yellow N_3−FeSOD adduct at 4.5 and 300 K (solid and dotted lines, respectively). Aside from the expected band sharpening at low temperature, the two sets of spectra are similar, suggesting that the yellow low-temperature adduct is analogous to the N_3−FeSOD species characterized crystallographically at physiological temperature.[5] On the basis of its high intensity and its absence in the spectrum of resting FeSOD (Figure 2, broken line), the prominent absorption feature at ~22 500 cm^{-1} has been assigned previously to an (N_3^-)-to-Fe^{3+} charge transfer (CT) transition.[16,34] Absorption and CD data were also obtained on an N_3−FeSOD sample that turns pink upon freezing (not shown). While the 300 K data are identical to those in Figure 2, the 4.5 K absorption spectrum of the pink species is red-shifted relative to the 300 K spectrum, indicating formation of a different species at low temperature.[35]

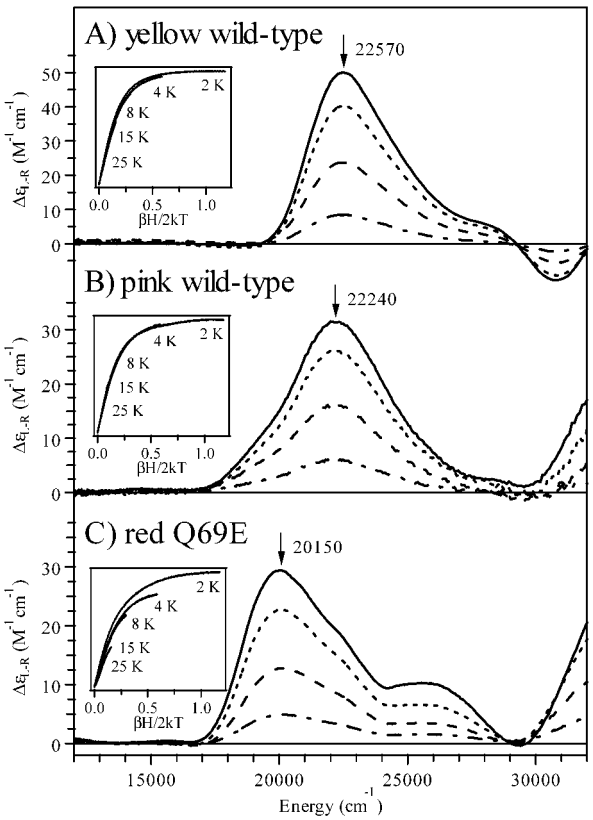

Figure 3. Variable-field (0.5, 1.5, 3.5, and 7 T) MCD spectra at 4.5 K of the yellow (A) and pink (B) wild-type N_3−FeSOD adducts and (C) the Q69E N_3−FeSOD complex. Insets: VTVH MCD data obtained at the positions indicated by arrows. Sample conditions: (A) [Fe^{3+}SOD] = 1.4 mM, [NaN_3] = 100 mM; (B) [Fe^{3+}SOD] = 0.25 mM, [NaN_3] = 50 mM; (C) [Q69E Fe^{3+}SOD] = 0.85 mM, [NaN_3] = 100 mM. Data were taken in 50% (v/v) glycerol and 50 mM phosphate buffer (pH 7.0).

MCD spectroscopy provides a particularly sensitive probe of the Fe^{3+} ligand environment in the yellow and pink N_3−FeSOD complexes (Figure 3, panels A and B). The similar energy and variable-temperature variable-field (VTVH) behavior of the dominant MCD feature in each spectrum, which coincides with the prominent (N_3^-)-to-Fe^{3+} CT transition in absorption, indicate that the yellow and pink species are similar in nature (i.e., spin Hamiltonian parameters and transition polarizations are nearly identical). Such similarities suggest that a single azide ligand is present in both species, contradicting a previous proposal invoking two N_3^- ligands in the pink species.[16]

To explore whether changes in the second coordination sphere are sufficient to produce the observed spectral differences between the yellow and pink N_3−FeSOD species, we have characterized the azide complexes of several second-sphere mutants of FeSOD. Consistent with the lack of a direct

(27) Vosko, S. H.; Wilk, L.; Nusair, M. *Can. J. Phys.* **1980**, *58*, 1200.
(28) Becke, A. D. *J. Chem. Phys.* **1986**, *84*, 4524−4529.
(29) Perdew, J. P. *Phys. Rev. B* **1986**, *33*, 8822−8824.
(30) Ridley, J.; Zerner, M. C. *Theor. Chim. Acta* **1973**, *32*, 111.
(31) Zerner, M. C.; Loew, G. H.; Kirchner, R. F.; Mueller-Westerhof, U. T. *J. Am. Chem. Soc.* **1980**, *102*, 589.
(32) Bacon, A. D.; Zerner, M. C. *Theor. Chim. Acta* **1979**, *53*, 21.
(33) Neese, F.; Solomon, E. I. *J. Am. Chem. Soc.* **1998**, *120*, 12829−12848.
(34) Averill, B. A.; Vincent, J. B. *Methods Enzymol.* **1993**, *226*, 33−51.
(35) Although glycerol disfavors formation of the pink N_3−FeSOD species upon freezing, we were able to prepare a glass of the pink adduct suitable for absorption and MCD experiments by systematically varying the protein and azide concentrations. As the CD data were distorted by glass strain, they are not considered here.

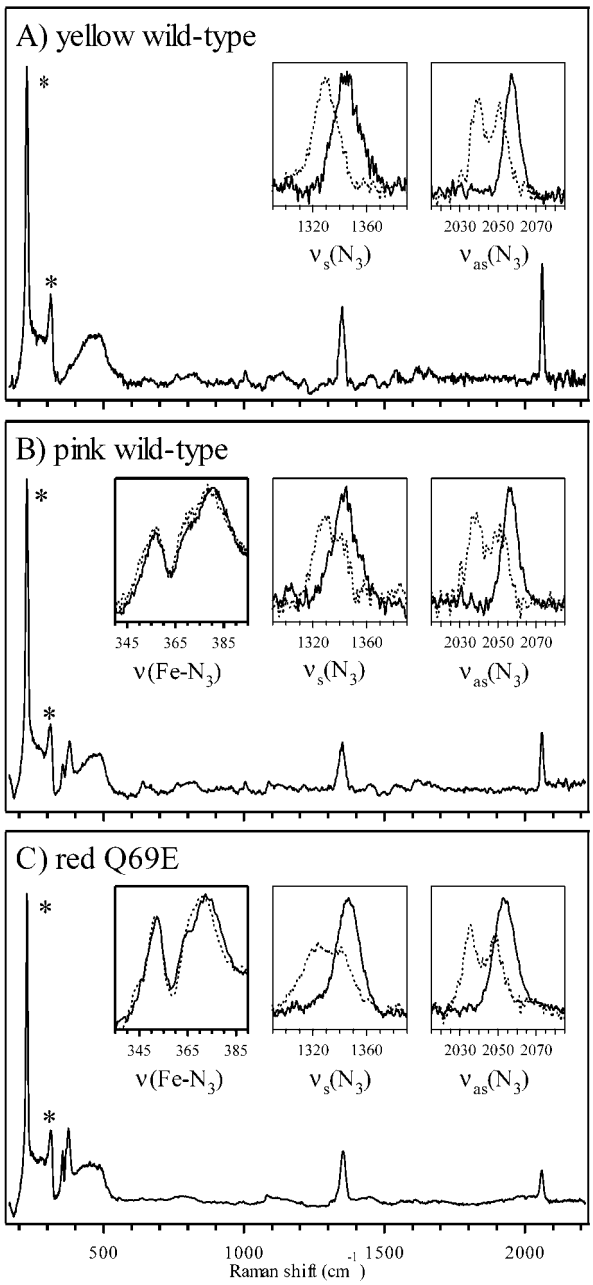

Figure 4. RR spectra at 77 K of the yellow (A) and pink (B) wild-type N_3−FeSOD adducts and (C) of the Q69E N_3−FeSOD species for 515 nm excitation. Ice peaks are indicated by asterisks. Insets: Expanded views of the protein-derived features for samples prepared with $^{14}N_3$ (solid lines) and ^{15}N-$^{14}N_2$ (dotted lines). Conditions: (A) [Fe^{3+}SOD] = 1.4 mM, [NaN_3] = 100 mM; (B) [Fe^{3+}SOD] = 0.25 mM, [NaN_3] = 50 mM; (C) [Q69E Fe^{3+}SOD] = 0.55 mM, [NaN_3] = 50 mM. All data were taken in 50 mM phosphate buffer (pH 7.0) using ∼20 mW laser power at the sample.

interaction between the second-sphere Gln69 and Fe-bound N_3^- in the wild-type protein (Figure 1),[5] the Q69E N_3-FeSOD MCD data (Figure 3C) are qualitatively similar to those obtained on the wild-type N_3−FeSOD species. Though some differences in VTVH MCD behavior are observed, simulations based on the formalism developed by Neese and Solomon[36] reveal that these differences can be ascribed primarily to a larger MCD *B*-term contribution to the mutant spectra; the spin Hamiltonian parameters and transition polarizations are indeed similar for all three species. However, despite the subtlety of the changes in the immediate metal-center environment upon Q69E mutation

Table 1. Peak Positions (in cm^{-1}) of the Azide-Related RR Features at 77 K for the Yellow and Pink Wild-Type N_3−FeSOD Adducts and for the Red Q69E Mutant N_3−FeSOD Species

FeSOD species	azide isotope	ν(Fe–N_3)	$\nu_s(N_3)$	$\nu_{as}(N_3)$
yellow wild-type	$^{14}N_3$	N/A	1345	2057
	^{15}N-$^{14}N_2$	N/A	∼1329	2039; 2051
pink wild-type	$^{14}N_3$	356; 368; 380	1345	2057
	^{15}N-$^{14}N_2$	355; 368; 378	1326; 1341	2038; 2051
red Q69E	$^{14}N_3$	355; 366; 376	1349	2054
	^{15}N-$^{14}N_2$	355; 367; 374	1327; 1346	2035; 2048

as revealed by MCD spectroscopy,[9] this perturbation is sufficient to shift the dominant (N_3^-)-to-Fe^{3+} CT transition by more than 2000 cm^{-1} to lower energy (Figure 3). As a result, the Q69E N_3−FeSOD species is red in color at all temperatures and all protein and N_3^- concentrations.

Vibrational Spectroscopy. The N_3−FeSOD adducts were further characterized using resonance Raman (RR) spectroscopy. Representative RR spectra obtained with 515 nm excitation are shown in Figure 4. In the RR spectra of the pink WT and red Q69E N_3−FeSOD species, SOD-derived features can be discerned near 370 (a group of three closely spaced components[37]), 1350 , and 2050 cm^{-1}. These features are shown on an expanded scale in the insets of Figure 4. While RR spectra obtained on the yellow N_3−FeSOD complex also display two prominent bands at 1345 and 2057 cm^{-1}, the lowest-energy feature is virtually absent. RR data obtained on Fe^{3+}SOD complexed with terminally ^{15}N-labeled azide (^{15}N-$^{14}N_2$) show downshifts and splittings of the two higher energy bands consistent with an end-on bound azide moiety and reveal that the highest energy component of the ∼370 cm^{-1} feature is also isotope sensitive (Figure 4, insets).

On the basis of a normal coordinate analysis (NCA) of the Fe−N_3 unit, the three isotope-sensitive bands are assigned to the Fe−N_3 stretch ν(Fe−N_3) and the symmetric and antisymmetric intra-azide stretches $\nu_s(N_3)$ and $\nu_{as}(N_3)$, respectively, in order of increasing energy (Table 1). The large splittings of the $\nu_{as}(N_3)$ features in the spectra of all N_3−FeSOD complexes prepared with ^{15}N-$^{14}N_2$ (Figure 4 and Table 1) reveal that the two intra-azide N−N stretch force constants k_{N-N} are inequivalent; our NCA yields k_{N-N} = 11.0 mdyn/Å (N−N bond adjacent to Fe−N bond) and 12.2 mdyn/Å (terminal N−N bond).

Thus, in each case we observe the RR features expected from the Fe−N_3 unit; however, variations in relative band intensities suggest differences in excited-state distortions along the Fe−N_3 and intra-azide coordinates and, therefore, differences in (N_3^-)−Fe^{3+} bonding. For the Q69E N_3−FeSOD species, a resonance Raman excitation profile for the Fe−N_3 and intra-azide stretches was obtained (not shown). All three azide-related features are strongly enhanced for laser excitation in resonance with the dominant absorption and MCD bands at ∼20 150 cm^{-1}, corroborating the assignment of this feature as an (N_3^-)-to-Fe^{3+} CT transition.[16,34] The three azide-related modes exhibit some qualitative differences in terms of their RR excitation behavior; that is, the ν(Fe−N_3) and $\nu_{as}(N_3)$ stretches are most strongly enhanced for excitation near 19 600 cm^{-1}, whereas the $\nu_s(N_3)$ stretch peaks around 20 600 cm^{-1}. This result suggests that the

(36) Neese, F.; Solomon, E. I. *Inorg. Chem.* **1999**, *38*, 1847−1865.
(37) Observation of three bands in the 350−400 cm^{-1} region suggests that the Fe−N_3 stretch is coupled to other modes, for example, other Fe−ligand stretches.

dominant MCD feature at ~20 150 cm^{-1} is actually composed of two components at ~19 600 and ~20 600 cm^{-1}, consistent with the asymmetric band shape of this feature and the calculations reported below, which also predict the presence of multiple (N_3^-)-to-Fe^{3+} CT transitions in that region.

Implications of the Spectroscopic Data. Our MCD and RR data (Figures 3 and 4) indicate that a single azide ligand is bound to the ferric centers of the three N_3−FeSOD complexes investigated. They also argue that the pink wild-type adduct does not correspond to a physical mixture of the yellow wild-type species and a red Q69E-like N_3−FeSOD form: (i) we were unable to satisfactorily model the MCD spectrum of the pink azide adduct in terms of a sum of the yellow and red N_3−FeSOD complex MCD spectra, and (ii) as the RR band positions vary between the yellow and red N_3−FeSOD complexes (Table 1), a physical mixture of these species would give rise to significantly broader Raman features. Yet, the widths of the Raman features of the pink form are not broadened (Figure 4). Additionally, EPR data reported in the literature reveal that by increasing the [N_3^-]/[Fe^{3+}SOD] ratio above 1, features associated with the yellow species gradually disappear concomitant with the appearance of new features associated with the pink form.[16]

A hint as to the structural differences between the three N_3−FeSOD species studied comes from the different azide orientations in the crystal structures of N_3−FeSOD and N_3−MnSOD (Figure 1).[5,11,12] An increase in γ from 117° to 147° is expected to reduce the σ-overlap between the azide π^{nb} orbital oriented in the Fe−N_3 plane and the Fe^{3+} 3d orbital directed toward azide, which consequently would weaken the (N_3^-)-Fe^{3+} σ-bonding interaction and lower the energy E_{CT} and intensity of the (N_3^-)-to-Fe^{3+} CT transition involving this pair of orbitals.

Computations. To establish a quantitative correlation between γ and E_{CT}, we have performed DFT and semiempirical INDO/S-CI calculations on N_3−FeSOD active site models that were obtained by replacing the Asp and His ligands with formate and amines, respectively. First, γ was increased in increments of 10° from 110° to 180°, and for each value the bond lengths of the Fe−N_3 unit were optimized through DFT energy minimizations. The lowest energy was obtained for $\gamma = 120°$, close to the experimental value of $\gamma = 117°$ in the yellow N_3−FeSOD complex characterized crystallographically.[5] Semiempirical INDO/S-CI computations were then performed on these DFT geometry-optimized models to calculate absorption spectra as a function of γ (Figure 5). A major advantage of the INDO/S-CI method relates to the fact that it permits reasonable estimates of transition energies and intensities for open-shell systems,[33] which is difficult to achieve using DFT computations. Additionally, INDO/S-CI calculations also yield ground-state spin Hamiltonian parameters that can be compared directly with experimental EPR data. To validate the use of this method, INDO/S-CI calculations were also performed on the Fe^{3+}SOD resting state for which extensive experimental data are available (i.e., spin Hamiltonian parameters have been reported in the literature,[38] and d−d as well as CT transition energies were obtained using MCD spectroscopy). Reasonable agreement was achieved between all experimental and calculated parameters.[39]

From an INDO/S-CI calculation on our N_3−FeSOD model with $\gamma = 120°$, a single (N_3^-)-to-Fe^{3+} CT transition contributing

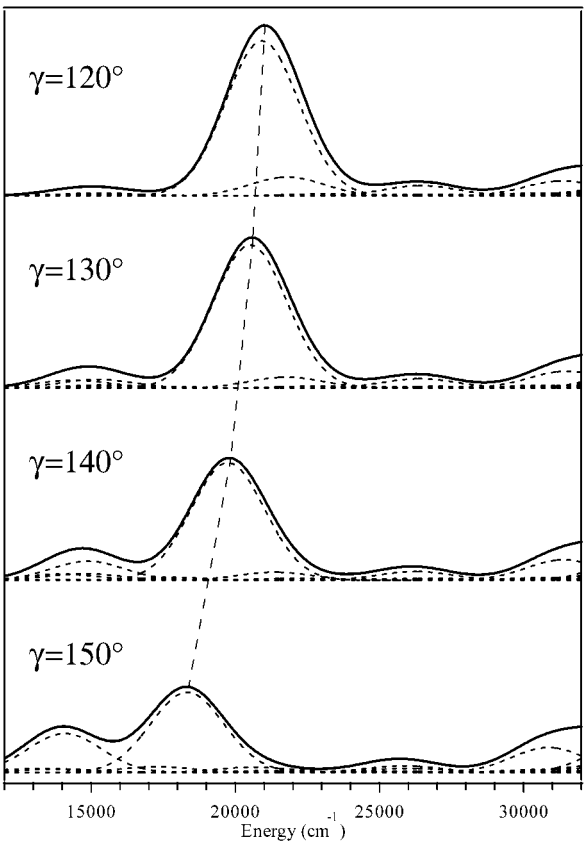

Figure 5. INDO/S-CI computed absorption spectra for a series of N_3−FeSOD active-site models that differ in terms of their Fe−N−N bond angles γ. All transitions contributing to the absorption envelopes (solid lines) are represented by Gaussian bands (dotted lines) that are scaled according to the calculated transition intensities. See text for details.

significant absorption intensity was obtained at 20 930 cm^{-1} (Figure 5), in good agreement with $E_{CT} \approx 22\,500$ cm^{-1} for the yellow N_3−FeSOD adduct (Figure 2) for which $\gamma = 117°$.[5] When γ was increased in increments of 10°, the calculated transition energy shifted to 20 520 (130°), 19 740 (140°), and 18 330 cm^{-1} (150°), and the intensity decreased gradually (Figure 5). Thus, our calculations reproduce the observed band shifts in Figure 3, supporting our model that the three azide adducts differ in terms of their Fe−N−N bond angles. For $\gamma >$ 140°, an additional (N_3^-)-to-Fe^{3+} CT transition, involving the other azide π^{nb} orbital, is expected to acquire significant absorption intensity near 14 000 cm^{-1} (Figure 5). As no such low-energy feature is observed experimentally (Figure 3), we estimate that $\gamma < 150°$ for all azide adducts included in our studies.[40]

In summary, combined DFT and INDO/S-CI calculations support our model that variation of a single parameter, the Fe−N−N angle γ, suffices to explain the differences in the electronic absorption and MCD spectra of the yellow, pink, and red N_3−FeSOD adducts. Possible implications of this result for the catalytic mechanisms of Mn- and FeSODs are discussed below.

4. Discussion

While the yellow and pink low-temperature N_3−FeSOD complexes have been known for more than two decades,[16] no geometric and electronic explanations of the spectroscopic

(38) Renault, J. P.; Verchere-Beaur, C.; Morgenstern-Badarau, I.; Yamakura, F.; Gerloch, M. *Inorg. Chem.* **2000**, *39*, 2666−2675.
(39) Jackson, T. A.; Brunold, T. C., unpublished results.
(40) Additional calculations were performed for $\gamma = 120°$ in which N_3^- was rotated about the Fe−N_3 bond axis. Changes in the calculated CT spectrum were relatively minor.

differences between the two forms have been proposed. Together, our spectroscopic and computational data suggest that both species possess a single, end-on bound azide ligand but differ with respect to their Fe−N−N bond angles γ. The two intra-azide N−N stretch force constants k_{N-N} obtained from our NCA on the Fe−N_3 unit are consistent with an $Fe^{3+}-N^{-}=N^{+}=N^{-}$ resonance structure.[10] Their inequivalence ($k_{N-N} = 11.0$ and 12.2 mdyn/Å) is relatively small, indicating that contributions from an $Fe^{3+}-N^{2-}-N^{+}\equiv N$ resonance structure are minor. Nevertheless, it is intriguing that the latter resonance structure, in which the Fe^{3+}-bound nitrogen carries more negative charge than the terminal nitrogen, does contribute to the ground-state electronic structure of the coordinated azide. By analogy, it might be anticipated that the Fe^{3+}-bound oxygen of the peroxide moiety in the putative peroxide−Fe^{3+}SOD intermediate[3] formed in the second half reaction (eq 2) also carries more negative charge than does the terminal oxygen. In this scenario, the peroxide ligand would be activated for protonation at the ligating oxygen rather than at the terminal oxygen. Protonation would then significantly weaken the Fe−hydroperoxide bond and promote product (HO_2^-) release.

On the basis of our computational data, we propose that an increase in γ by ~10° is sufficient to account for the observed color change from yellow to pink upon freezing of wild-type N_3−FeSOD solutions. While our data indicate that a single azide ligand is also present in the pink azide complex, formation of this species only when $[N_3^-]/[Fe^{3+}SOD] > 2$[16] suggests that a second N_3^- molecule could be bound to the FeSOD protein at a substrate prebinding site.[41] The nature of this putative prebinding site can be inferred[8,42,43] from the crystal structure of FeSOD, which shows a solvent molecule only 3.3 Å away from the phenolic O of the second-sphere Tyr at position 34.[5] As this Tyr is part of the highly conserved H-bond network that includes Gln69 and the metal-bound solvent ligand (Figure 1), steric and electrostatic changes associated with N_3^- incorporation into the prebinding site could be propagated through the H-bond network to perturb the $(N_3^-)-Fe^{3+}$ bonding interactions.[44] Support for this model is provided by our data on Q69E N_3−FeSOD, where perturbation of this H-bond network gives rise to substantial changes in positioning of the azide ligand (i.e., γ increases by ~20° upon mutation of Gln69 to Glu).

The above findings suggest that the second coordination sphere may play an important role in orienting the incoming substrate $O_2^{\bullet-}$ for reaction with the FeSOD active site. Notably, the strongest Fe−N_3 σ-bonding interaction is calculated for $\gamma = 120°$, close to the value of $\gamma = 117°$ observed for the yellow N_3−FeSOD adduct at physiological temperature.[4] This bonding interaction can be inferred from the unoccupied spin-down MO derived from the Fe^{3+} 3d orbital that is pointing toward the in-plane azide π^{nb} orbital (Figure 6). As this MO is unoccupied, contributions from the azide π^{nb} orbital are due to delocalization of hole character from Fe^{3+} to azide and reflect the amount of

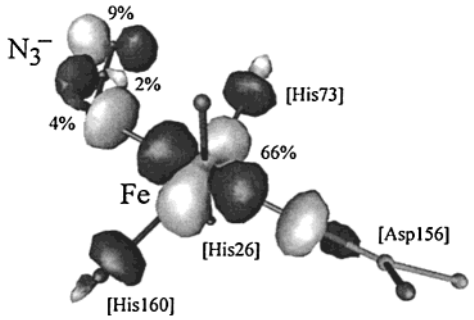

Figure 6. Boundary surface plot of the unoccupied spin-down MO derived from the Fe^{3+} 3d orbital that is pointing toward the azide π^{nb} orbital oriented in the Fe−N_3 plane. Contributions from the Fe 3d and azide N 2s,2p orbitals are indicated. The His and Asp ligands were modeled by amines and formate, respectively.

$N_3^- \rightarrow Fe^{3+}$ charge donation in the azide π^{nb}-derived occupied MO. Consistent with the findings from our NCA on the Fe−N_3 unit, our DFT calculations also suggest that the Fe^{3+}-bound nitrogen carries more negative charge than does the terminal nitrogen, as the latter produces the largest azide contribution to the Fe 3d-derived unoccupied MO in Figure 6. Hence, by orienting the substrate molecule in a similar way, the second coordination sphere could (i) ensure large electronic coupling between $O_2^{\bullet-}$ and Fe^{3+}, thereby reducing the Franck−Condon barrier to electron transfer, and (ii) promote protonation of the oxygen that coordinates to Fe^{3+}, thus facilitating HO_2^- release in the second half reaction (eq 2) of the catalytic cycle.

Given the likely importance of proper substrate orientation for maximum SOD activity, the very different metal−N−N bond angles in the crystal structures of N_3−MnSOD and N_3−FeSOD (Figure 1) are intriguing and raise the questions of the origin and the possible mechanistic implications of this structural difference. Because of the different electron configurations of Mn^{3+} ($3d^4$) and Fe^{3+} ($3d^5$), the metal 3d-based redox-active orbitals of the Mn- and FeSOD active sites that accept an electron from $O_2^{\bullet-}$ in the first step of the catalytic cycle (eq 1) are very different in nature, that is, σ- and π-antibonding, respectively, with respect to metal−ligand (or substrate) bonds.[39] Hence, differences in the second coordination spheres of the Mn- and FeSOD proteins (e.g., positioning of Gln146/69, Figure 1), previously shown to be crucial for adjusting the E_m of the bound metal ion,[7,9,17] might also impose different orientations on the incoming substrate to maximize overlap of the $O_2^{\bullet-}$ π^* orbital with the appropriate metal 3d-based redox active orbitals. This issue is currently being addressed through combined spectroscopic/computational studies on the metal-substituted SODs and their interaction with substrate analogues.

Acknowledgment. A.-F.M. acknowledges financial support by The Petroleum Research Fund (ACS-PRF 33266-AC4,3), administered by the ACS, the Commonwealth of Kentucky Research Challenge Trust Fund, N.I.H (GM55210), and N.S.F. (MCB9728793). T.C.B. thanks the University of Wisconsin for generous support, Jennifer Craft for valuable discussions, and Dr. Frank Neese (MPI Mülheim) for a free copy of his ORCA 2001 software package and for his help with INDO/S-CI calculations.

Supporting Information Available: Experimental details (PDF). This material is available free of charge via the Internet at http://pubs.acs.org.

JA016254H

(41) Our data argue against similar N_3^- orientations in the pink N_3−FeSOD species and N_3−MnSOD: (i) an H-bond with Tyr34 would perturb intra-azide bonding, yet our normal coordinate analysis yields similar intra-azide force constants for all azide adducts, and (ii) in the Q69E N_3−FeSOD adduct, the phenolic Tyr34 proton is presumably involved in H-bonding to Glu and thus unavailable for H-bonding to azide.

(42) Vathyam, S.; Byrd, R. A.; Miller, A.-F. *Magn. Reson. Chem.* **2000**, *38*, 536−542.
(43) Sorkin, D. L. Ph.D. Thesis, The Johns Hopkins University, 1999.

(44) The fact that glycerol disfavors formation of the pink N_3−FeSOD species could thus be explained in terms of a competition between glycerol and N_3^- for the putative prebinding site.